ACS APPLIED NANO MATERIALS
Cite This: ACS Appl. Nano Mater. 2018, 1, 6073−6080
Article
www.acsanm.org

Poly(1-vinyladamantane) as a Template for Nanodiamond Synthesis

Matthias Spohn,[†] Masfer H. A. Alkahtani,[§] Robert Leiter,[‡] Haoyuan Qi,[‡] Ute Kaiser,[‡] Philip Hemmer,[§,∥,⊥] and Ulrich Ziener*[,†]

[†]Institut für Organische Chemie III, Makromolekulare Chemie, and [‡]Zentrale Einrichtung Elektronenmikroskopie, Arbeitsgruppe Materialwissenschaftliche Elektronenmikroskopie, Universität Ulm, Albert-Einstein-Allee 11, D-89081 Ulm, Germany

[§]Electrical & Computer Engineering Department (ECEN) and [∥]The Institute for Quantum Science and Engineering (IQSE), Texas A&M University, College Station, Texas 77843, United States

[⊥]Zavoisky Physical-Technical Institute, Federal Research Center "Kazan Scientific Center of RAS", 420029 Kazan, Russia

Supporting Information

ABSTRACT: The cationic polymerization of 1-vinyladamantane with various initiating systems was studied, and the resulting polymer was characterized. During this work, a new initiating system was found for the cationic polymerization of sterically demanding monomers like 1-vinyladamantane. A sample was successfully employed as a template for nanodiamond synthesis in a diamond anvil cell under moderate temperature and high pressure.

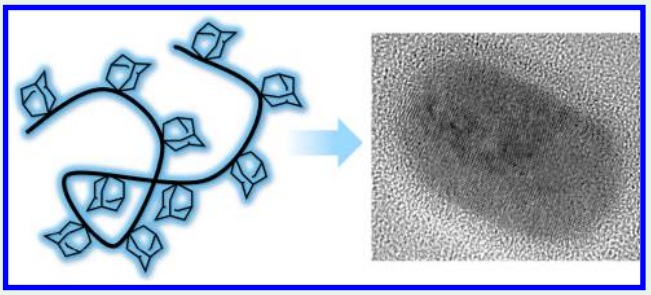

KEYWORDS: *nanodiamonds, polymer, template, adamantane, cationic polymerization, initiator*

INTRODUCTION

Diamondoids are molecules consisting of a few lattice units of the cubic face-centered diamond lattice and already show some of the properties of macroscopic diamond.[1] These are, for example, exceptional mechanical, thermal, and chemical stability.[2] Diamondoids can be seen as nanometer-sized, hydrogen-terminated diamonds, with adamantane as the smallest representative of this class.

The production of diamond materials is often based on templating processes. For example, nanodiamonds generated by detonation are frequently employed for the formation of diamond thin films.[3] Molecular seeds as templates for nanodiamond synthesis are also described. As a small part of the diamond lattice adamantane and its higher homologues (oligo- and polymantanes) are, in principle, well suited as such molecular seeds for nucleation enhancement. One-dimensional analogues of nanodiamonds could be achieved by the templating with 4,9-dibromodiamantane inside carbon nanotubes as confined space.[4] Chen et al.[5,6] and Melosh[7] have reported on chemical vapor deposition (CVD) growth of nanodiamonds from diamondoid seeds attached to different substrates like monocrystalline silicon or sapphire. Without covalent attachment, a major drawback of small molecule seeds is their high evaporation rate at elevated temperatures as reached during CVD processes.[8] Also in homogeneous phase synthesis under high pressure and high temperature (HPHT) the nucleation efficiency by the statistically distributed seed molecules can be hardly controlled. These problems can be circumvented by employing polymeric seeds. Best suited should be all-carbon polymers because they reduce the likelihood of defects in the generated diamond lattice due to the incorporation of foreign elements. Additionally, the sp^3-carbon chain of the polymer backbone is expected to be sufficiently thermally stable to withstand the elevated temperatures in the nanodiamond synthesis processes. The simplest vinyl monomer containing adamantane is 1-vinyladamantane. A poly(1-vinyladamantane) molecule of sufficient length should show negligible evaporation, making it an attractive candidate for seeded nanodiamond growth by CVD or related processes.

Until now there are only two reports on the polymerization of 1-vinyladamantane by Žuanić et al.[9] and Robello.[10] Both used aluminum bromide as initiator in a cationic polymerization. Žuanić et al.[9] demonstrated the formation of the target polymer by nuclear magnetic resonance (NMR) spectroscopy and employing 10 mol % of initiator. Unfortunately, this polymer displayed rapid degradation above 300 °C.[9] Robello[10] examined the polymer resulting from a similar polymerization with only 1 mol % of aluminum bromide. The insoluble part in dichloromethane was removed, and the remaining polymeric material showed a molar mass between 390 and 610 g mol^{-1} determined by gel permeation chromatography (GPC). This corresponds to a short average chain length between dimer and tetramer, which suggests the presence of oligomers rather than polymers.

Received: July 20, 2018
Accepted: October 22, 2018
Published: October 22, 2018

DOI: 10.1021/acsanm.8b01238
ACS Appl. Nano Mater. 2018, 1, 6073−6080

It is striking that no other initiating systems for the polymerization of this simple monomer have been reported. In general, there is a broad variety of potential initiators for cationic polymerization. The reactive carbocation on a vinyl monomer is usually generated using various acids as initiators. In combination with more reactive monomers even proton acids like sulfuric acid can be used. In this case the monomer is initiated by proton addition to the double bond. The possibility of the addition is thereby directly linked to the acidity of the initiator. Also, a whole range of Lewis acids like titanium,[11] vanadium, aluminum,[12] tin,[13] or boron[14−16] containing halides, alkoxides, and so forth can be employed. There are two possible initiating mechanisms for Lewis acids commonly discussed in textbooks.[17] The first possibility is the direct initiation by self-ionization of the Lewis acid. In the case of aluminum bromide $AlBr_2^+$ and $AlBr_4^-$ are formed in situ, and the cation generates the active species while the anion acts as a weakly binding counterion to stabilize the reactive chain-end. The second possibility is assumed to be the more common initiating mechanism. Here, the Lewis acid reacts with a proton-containing co-initiator forming a very weakly nucleophilic anion and a highly acidic proton, which then initiates the polymerization. Common co-initiators are foremost water, which is nearly always present and hard to completely remove from any system, but also strong proton acids like trifluoroacetic acid (TFA) or trifluoromethanesulfonic acid (TfOH) are used for unreactive monomers.

Employing polymers as templates for the synthesis of nanostructured materials requires a very good control over the polymer synthesis as subtle changes of molecular structures (molecular weight and distribution) might strongly affect the templating process. Motivated by the surprisingly low reactivity of the monomer and the huge amounts of initiator required for polymerization,[9,10] we report the investigation of the cationic polymerization of 1-vinyladamantane focusing on the variation of the initiators. Molar masses of the soluble part in organic solvents of up to 2400 g mol^{-1} could be obtained, as determined by GPC. This molar mass corresponds to an average chain length of 15 repeating units. The molar masses are additionally confirmed by an internal calibration of the GPC elugram. Furthermore, of the initiators used, the kinetics with $AlBr_3$ are investigated in detail, and a system based on $TiCl_4$ and TfOH is reported for the first time. Finally, a representative polymer sample is employed as a template for nanodiamond synthesis under high pressure/moderate temperature (HPMT).

EXPERIMENTAL SECTION

General. The NMR measurements were recorded on a Bruker Avance 400 NMR spectrometer with $CDCl_3$ as solvent (400.13 MHz). The solvent residue peak ($CDCl_3$, δ = 7.26 ppm) was used as internal standard, and the signals were given in parts per million. IR spectra were recorded on a Bruker Vertex 70 IR spectrometer with an ATR unit in a wavenumber region of 550−4000 cm^{-1}. The GPC measurements were done on an Agilent 1260 Infinity GPC/SEC device with a (PSS) SDV linear M 5 μm column in THF as eluent. To increase the detected signals, sample concentrations of 10 mg mL^{-1} were used, and 100 μL sample solution were injected with every run. The molecular weights are given compared to polystyrene standards of various degrees of polymerization. The signals were detected via a refractive index detector. CI-MS spectra were recorded on a Finnigan SSQ-700. For the TGA measurements a SDTA851^e device from Mettler-Toledo was used with a heating rate of 10 °C min^{-1}. The DSC measurements were done on a DSC 2 STAR^e system from Mettler-Toledo with a heating rate of 10 °C min^{-1} for the examination of a possible melting point and with a heating rate of 50 °C min^{-1} for the measurement of the glass transition temperature. The solvents and reactants were carefully dried according to a literature procedure with a suitable desiccant[18] and stored under strictly inert conditions. The reactions were all performed in a flame-dried Schlenk flask under argon. 1-Vinyladamantane was prepared according to the literature.[19]

Synthesis of $TiCl_2(OTf)_2$. $TiCl_2(OTf)_2$ was prepared by the slow addition of 600 mg of TfOH (4.0 mmol, 2.0 equiv) to 379 mg of $TiCl_4$ (2.0 mmol, 1.0 equiv) in DCM at 0 °C, similar to the literature synthesis.[20] The resulting precipitated yellow solid was dried in a vacuum and directly used as initiator.

Polymerization. All polymerization reactions were performed under standardized conditions. In an exemplary reaction 162 mg of 1-vinyladamantane (1.0 mmol, 1.0 equiv) was mixed with 3 mL of dry dichloromethane under inert conditions. The solution was then either used at room temperature or cooled to −78 °C in an acetone−dry ice bath. 26.7 mg of aluminum bromide (0.1 mmol, 0.1 equiv) was added, and the yellow reaction mixture was either stirred at −78 °C for 4 h before slow warming to ambient temperature and further stirring for 16 h or it was stirred for 18 h at room temperature. Afterward, the active species was terminated with 10 mL of methanol, and the formed polymer precipitated simultaneously. The precipitate was centrifuged off, and the supernatant was separated. The polymer was washed with methanol, dried for 4 h at 80 °C, and obtained as a white powder. It was characterized by NMR spectroscopy and GPC in THF. The supernatant, containing residual monomer and oligomers, was mixed with 11 mL of a 10:1 mixture of saturated aqueous ammonium chloride solution and water. The aqueous phase was extracted three times with 15 mL of *n*-hexane each, and the mixed organic phases were dried over $MgSO_4$. The solvent was removed, and the residue was characterized by NMR spectroscopy and GPC in THF. Tables S1 and S2 summarize the reaction conditions and resulting amounts and molecular weights of the isolated polymer and oligomer fraction, respectively. Representative spectral data of a sample are given below.

^{1}H NMR (see Figure S1b) (400 MHz, $CDCl_3$, 20 °C) δ [ppm] = 5.26−5.01 (br, 2H, CH═CH end-groups), 2.30−1.93 (m, 3H, CH (Ad), 1.68−0.76 (m, 15H, CH_2(Ad) + CH (backbone) + CH_2 (backbone)).

MS (CI) (see Figure S2): 135 $[M - C_2H_3]^+$, 163 $[M + 1]^+$, 297 $[2M - C_2H_3]^+$, 325 $[2M + 1]^+$, 459 $[3M - C_2H_3]^+$, 487 $[3M + 1]^+$, 621 $[4M - C_2H_3]^+$, 650 $[4M + 1]^+$, 784 $[5M - C_2H_3]^+$, 812 $[5M + 1]^+$.

IR (KBr) (see Figure S3): 2900 (ν(CH)), 2840 (ν(CH)), 1450 cm^{-1} (δ(CH) ip).

Seeded Diamond Growth Procedure. In addition to the purification described above and to ensure a minimum amount of impurities in the template polymer for diamond growth, the polymer sample was washed with a mixture of methanol/conc HCl_{aq} 10:1 (v:v) and centrifuged. The solid residue was dissolved twice in a minimum amount of *o*-dichlorobenzene and precipitated with methanol. The resulting white powder was washed with methanol and dried for 4 h at 80 °C. The experimental procedure used to grow nanodiamonds around polymer chains of adamantane molecules is similar to that used to demonstrate growth of nanodiamond around adamantane molecules.[21] Briefly, the starting material was placed in a diamond anvil cell (DAC) and pressurized to 7 GPa, and the entire DAC was heated to temperatures of 275 °C or lower in an oven for maximum of 18 h.

The growth mix consisted mainly of saturated hydrocarbons heptamethylnonane ($(CH_3)_3CCH_2CH(CH_3)CH_2C(CH_3)_2CH_2C(CH_3)_3$, Sigma-Aldrich, >98%) and tetracosane ($(CH_3(CH_2)_{22}CH_3)$, Sigma-Aldrich, >98%), plus a small amount of the polymer seed molecule. Typical formulations were poly(1-vinyladamantane) (1 mg) + heptamethylnonane (200 μL) + tetracosane (2 mL) + tetramethylhydrazine (10 μL). A small amount of the growth mix

DOI: 10.1021/acsanm.8b01238
ACS Appl. Nano Mater. 2018, 1, 6073−6080

was transferred into the 100 μm diameter sample chamber (gasket) placed between two diamond anvils in the DAC.

After growth, the sample was then extracted from the diamond anvil cell by a needle with a 2 μm tip (American Probe Technologies, Inc.). To ensure a successful transfer of nanodiamonds from the growth chamber, we dip the tip of the extraction needle into 200 μL of an isopropanol/ethanol solution, repeating several times until the growth chamber is emptied. For TEM and optical characterization a few drops of the nanodiamond solution was placed on a lacy carbon TEM grid. This prepared grid was then baked in a vacuum to 800 °C for about 20 min to evaporate unwanted byproducts from the reaction mixture.

Electron Microscopy. HRTEM imaging was performed using the C_c/C_s-corrected Sub-Angstrom Low-Voltage Electron (SALVE) microscope operated at 60 kV. The chromatic and spherical aberration coefficients, i.e., C_c and C_s, were tuned to −20 μm and −15 μm, respectively. A Ceta 16M camera (FEI) was applied for image acquisition.

RESULTS AND DISCUSSION

The synthesis of the monomer 1-vinyladamantane is reported several times in the literature, but mostly with a quite poor yield.[19] Fokin et al.[19] established an efficient method for the preparation by elimination of HBr from (2-bromoethyl)-1-adamantane. This was followed in the present work with good total yields of 86% for the synthesis of the monomer.

Polymer Synthesis and Characterization. The polymerization of 1-vinyladamantane was performed under various conditions as illustrated in Figure 1. The success of

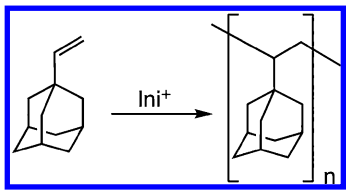

Figure 1. General reaction scheme of the cationic polymerization of 1-vinyladamantane.

polymerization was determined by the amount of solid precipitate formed under addition of methanol to the reaction mixture in dichloromethane. Oligomers and unreacted monomer were determined in the supernatant by ^{1}H NMR spectroscopy. In the following the term polymer refers to the precipitate washed once with methanol, and oligomer means the solute of the combined methanol solutions. The sample for nanodiamond synthesis was further washed to reduce the organic and inorganic impurities to a minimum (see the Experimental Section).

Starting from the literature-known initiator aluminum bromide, various other common cationic initiating systems were tested during the course of this work. Aluminum chloride was found to be slightly less reactive than the corresponding bromide, which can be explained by the somewhat lower acidity of the chloride.[22] Additionally, the tetrabromoaluminate, which is formed during the initiation step, is a weaker binding counterion compared to the corresponding chloro compound because of its larger size. Therefore, the cation at the polymer chain-end is less stabilized and remains more reactive. Other weaker Lewis acids, which are commonly used as initiators for cationic polymerizations, like for example iron(III) chloride, tin(IV) chloride, or boron(III) bromide, showed no polymerization. The initiation with strong proton acids like trifluoromethanesulfonic acid or trifluoroacetic acid did not lead to polymers either. This suggests that only the strongest acids combined with very weakly binding counterions are suited as initiators (Table 1). Therefore, other equally

Table 1. Different Possible Initiators for the Polymerization of 1-Vinyladamantane[a]

initiator	T = −78 °C	T = rt
$AlBr_3$	x	x
$AlCl_3$	x	x
SbF_5	x	x
$TiCl_4$	o	o
$ZrCl_4$	o	o

[a]The reactions were all carried out with 10 mol % initiator in DCM at −78 °C and at room temperature. x = polymer was obtained; o = oligomer was obtained.

strong or even stronger acids than aluminum bromide were selected. Foremost among them is the superacid antimony(V) fluoride, which also initiated the polymerization in good yields. However, similar initiators like titanium(IV) chloride and zirconium(IV) chloride only yielded short oligomers.

Generally, at lower reaction temperatures higher degrees of polymerization were obtained for polymers soluble in THF. This is in good agreement with a significant decrease in the rate of chain-transfer and termination reactions compared to the propagation reaction at lower temperatures. The polymeric material produced at −78 °C was normally completely soluble in THF whereas the material obtained from the reaction at room temperature contained a large part, which is insoluble in common organic solvents. Presumably, this part consists of cross-linked polymer with a strongly reduced solubility. In the material produced at −78 °C with SbF_5 as initiator the longest soluble polymers with an average molecular weight of about 2400 g mol^{-1} were found. But this material also contained an insoluble part despite the low reaction temperature. This is attributed to the very weakly binding SbF_6^- anion, which generates a highly reactive cation favoring chain-transfer reactions presumably of hydride (see below) even at low temperatures. These chain transfer reactions probably lead to branched or cross-linked polymers.

With 10 mol % $AlBr_3$ as initiator polymer with an average molecular weight of around 1500 g mol^{-1} was obtained at −78 °C. This corresponds to an average chain length of 9−10 monomer units, which is in good agreement with the monomer−initiator ratio. In contrast, the same reaction at room temperature yielded material with an M_n of only 540 g mol^{-1}. It should be noted that the molecular weight is determined only for the shorter, soluble in THF, chains probably underestimating the average molar mass of the total sample. To synthesize higher molecular weight polymer, the initiator concentration was decreased, but with 1 and 5 mol % only up to 17% of polymer could be isolated. The assumption that the low yield is caused by contaminations due to the small scale of the reaction could not be confirmed as doubling the scale of the reaction still resulted in only 18% polymer yield. The low conversion at a low concentration of initiator could also be caused by the precipitation of active polymer chains at an early stage of polymerization before chain transfer reactions take place, thereby removing the active cations from the reaction solution. If the polymer chains with more than 15−20 monomer units are insoluble, then 1 mol % initiator can only yield 10%−20% polymer, which is in good agreement with the

DOI: 10.1021/acsanm.8b01238
ACS Appl. Nano Mater. 2018, 1, 6073−6080

findings above. The degree of polymerization, above which the polymer is insoluble, is difficult to determine but should not be much higher than 15 units because little polymer of more than 2400 g mol^{-1} was found in GPC measurements in THF, and the polymer solubility in DCM is even lower.

The active species during the polymerization is intensely yellow. For 1-vinyladamantane, no obvious stabilization of the active species (cation) by delocalization is expected in contrast to ionic polymerizations of other monomers like styrene or acrylates which could give rise to the intense color. We surmise that a colored complex is formed between the initiated monomer and the weakly binding counterion. Even at low initiator concentrations of 1% or 2% and with some poor initiating systems, the same species is observed. This indicates that the active species is formed, but the polymerization does not proceed quantitatively. With 20 mol % of initiator very short oligomers were formed because statistically only pentamers can be obtained with this initiator concentration. Therefore, 10 mol % of initiator was used as standard conditions to determine the activity of all other initiating systems.

Besides the absolute amount, the concentration of monomer was varied, too. It turned out that a monomer concentration of 0.33 mol L^{-1} is optimal with a yield of up to 90% polymer. Both lower (0.17 mol L^{-1}) and higher concentrations (0.67 mol L^{-1}) resulted in negligible polymer yields. The finding at higher monomer concentration might be attributed to the lower solubility of the polymer in this monomer−DCM mixture, which would then lead to earlier precipitation of the polymer at quite low conversion (see above). At lower monomer concentration, the propagation is much slower and termination reactions might predominate.

Although the single-component initiators, titanium[IV] chloride or zirconium[IV] chloride (Table 1), did not yield any or no significant amounts of polymer, the combination of these with trifluoromethanesulfonic acid (TfOH) or trifluoroacetic acid (TFA) showed promising behavior (Table 2). The

Table 2. Acid-Promoted Polymerization of 1-Vinyladamantane with Different Titanium Group Elements and SbF_5 in DCM[a]

initiator	c [mol %]	T = −78 °C	T = rt
$TiCl_4$ + TfOH	10 + 10	x	x
$TiCl_4$ + TfOH	10 + 1	nd	o
$TiCl_4$ + TfOH	1 + 10	nd	x
$TiCl_2(OTf)_2$	10	x	x
HCl	10	−	nd
HCl + $TiCl_4$	10 + 10	−	nd
HCl + $TiCl_4$ + NaOTf	10 + 10 + 10	o	nd
$TiCl_4$ + NaOTf	10 + 10	o	o
$TiCl_4$ + TFA	10 + 10	nd	o
$ZrCl_4$ + TfOH	10 + 10	o	x
SbF_5 + TfOH	10 + 10	x	x

[a]x = polymer was obtained; o = oligomer was obtained; − = no conversion (monomer regained); nd = not determined.

Lewis acids alone mainly deliver oligomer at room temperature. At −78 °C the yield is even further decreased. Together with a very strong Brönsted acid, polymer is formed in different amounts depending on the temperature and the ratio of Lewis and Brönsted acid, respectively. The latter reacts in situ with the Lewis acid, leading to formation of an even more acidic compound with a bulky counterion. This strong acid then initiates the reaction. Alternatively, the initiator can be synthesized beforehand and added afterward to the reaction mixture. The reaction of $TiCl_4$ and TfOH gives the mixed complex $TiCl_2(OTf)_2$ under HCl evolution as a bright yellow solid.[20] In the solid state under normal conditions $TiCl_2(OTf)_2$ is the most stable mixed complex.

To elucidate the role of the involved species of this system and to get a deeper insight into the initiation mechanism, the different components were examined separately (Table 2). HCl and $TiCl_4$ alone show no polymerization, but in combination with sodium triflate oligomers are formed. The most efficient initiator in our experiments was formed with a 1:1 ratio of $TiCl_4$ and TfOH. However, it is possible to use one component in excess, like a 1:10 ratio of $TiCl_4$ and TfOH, but the reverse ratio is not favorable. This is attributed to the excess of TfOH supporting the formation of the active complex.

Generating the initiator by ion exchange from $TiCl_4$ and NaOTf is less efficient than by reaction of $TiCl_4$ with TfOH because the evolution of HCl, in the second case, shifts the equilibrium quantitatively toward $TiCl_2(OTf)_2$. This species will act as a very strong Lewis acid delivering a spatially highly demanding counterion, which is crucial for the successful cationic polymerization.

Although titanium species are well-known catalysts for insertion polymerization, a coordinative mechanism is, in the present case, unlikely as specific tests to polymerize 1-vinyladamantane with Ziegler−Natta catalysts have failed. The activity of $ZrCl_4$ and TfOH shows that this reactivity is common within the titanium group elements, although $ZrCl_4$ is less active. The difference in reactivity between both chloro complexes can be explained by the higher acidity of titanium due to its smaller ion radius. Instead of the triflic acid, TFA can be employed to form an acidic complex with $TiCl_4$ which acts as an initiator, too, but less efficient (Table 2).

For comparison with other cationic polymerizations, we determined the kinetics of the reaction in one exemplary case. Although there is no direct proof for a living nature of the present polymerizations, ideal conditions of a living polymerization were assumed for simplicity reasons. This leads to an exponential expression (eq 1) for the conversion over time (see the Supporting Information for details).

$$C(t) = -C_{max} e^{-k_p[I]t} + C_{max} \quad (1)$$

The conversion was determined by taking samples from a standard polymerization reaction after various time intervals and measuring the polymer mass after washing and drying under high vacuum. The reaction was performed at −78 °C and with 10 mol % aluminum bromide as initiator in DCM. The samples were terminated with a base (aniline) in DCM. Figure 2 shows the conversion of the reaction over time. The maximum conversion is reached very fast because of the high initiator concentration compared to common cationic polymerizations. For longer times the deviation of the maximum conversion from quantitative conversion is probably caused by losses during the washing and drying process and inaccuracies in the sample taking process.

From the nonlinear fit in Figure 2 a propagation constant of 2.5 ± 1.3 L mol^{-1} s^{-1} can be derived. The constant is in a comparable range as for cationic polymerizations of other monomers, although a reliable comparison is challenging because of the strong dependence on the solvent and reaction

DOI: 10.1021/acsanm.8b01238
ACS Appl. Nano Mater. 2018, 1, 6073−6080

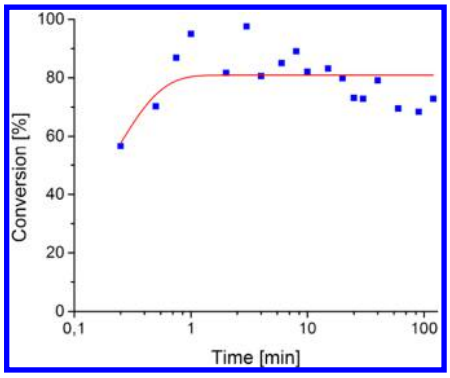

Figure 2. Experimental conversion of the polymerization of 1-vinyladamantane with 10 mol % aluminum bromide at −78 °C in DCM over time and the exponential fit function (eq 1).

temperature. At −30 °C styrene shows a propagation constant of 0.7 L mol^{-1} s^{-1} in DCM[23] and the better stabilized isobutyl vinyl ether a corresponding value of 6.3 L mol^{-1} s^{-1} in ethylene chloride.[24] Following the general trend over the temperature reported in the literature,[23] the corresponding rate constants at −78 °C should be even lower.

In the ^{1}H NMR spectra of both the oligomer (Figure S1a) and the polymer (Figure S1b), mostly weak signals around 5.1 ppm are found besides the expected signals between 0.8 and 2.3 ppm typical for the adamantane unit and the aliphatic backbone. The signals between 1.9 and 2.3 ppm are tentatively assigned to the adamantane bridging CH_2 groups next to the polymer backbone while the other signals between 0.8 and 1.7 ppm are originating from the remaining adamantane protons and the polymer backbone, respectively (Figure S1b). The integrals of both groups with a ratio of 3:15 as expected for the intact polymer suggest the absence of side reactions. But traces of, for example, rearranged species via stabilized cationic intermediates in the adamantane scaffold by hyperconjugation, potentially caused by the effect of the strong Lewis acid initiator, cannot be excluded.[25] Different conformations of the sterically constrained polymer backbone and restricted rotation of the adamantane units might further complicate the spectra[26] and make an conclusive assignment of the peaks and precise determination of the polymer structure difficult. Additional little peaks between 3 and 6 ppm in the spectrum of the polymer washed only once vanish after further careful washing probably because of small molecule impurities. The low field signals in the purified polymer are attributed to olefinic protons but not to traces of residual monomer which displays in addition characteristic peaks at ca. 4.8 ppm. The latter are not present anymore in the polymer (Figure S1b). Thus, we assume that the olefinic moiety arises from end-groups which are presumably caused by termination via elimination. In the literature[17,27] elimination is discussed as termination or transfer reaction for cationic polymerization. The spectra of some polymer samples additionally show a weak signal at 3.5 ppm (see Figure S1c), which might indicate the presence of hydroxy end-groups resulting from a quenching with water. From the integral ratios of the olefinic and aliphatic proton signals a degree of polymerization (DP) of around 10 can be roughly estimated. This is in the same order as determined by GPC (see below). The poor signal-to-noise ratio prevents an exact quantification of DP, and in addition, polymer chains with alkyl end-groups cannot be excluded. In this case, the active chain might have been terminated by a hydride transfer from solvent molecules (DCM). A hydride transfer reaction is known in the literature for trioxane as monomer.[28] Despite the addition of potential quenching agents like aniline, triethylamine, methanol, or various halogen ions to the reaction mixture, no hints of other end-groups than the above-mentioned ones could be detected. Presumably, the strong sterical hindrance at the chain-end, due to the large adamantane moieties in the side chains, prevents efficient attack by the nucleophiles. The IR spectra are in accordance with the expected structure of the aliphatic backbone with pending adamantane moieties reflected by stretching and deformation vibrations of the methylene and methine groups, respectively (Figure S2). There are no hints to (olefinic) end-groups because of their low concentration.

For GPC measurements, the soluble portions of the polymers in THF were investigated. Although THF, toluene, and especially halogenated aromatic compounds proved to be good solvents, the material polymerized at room temperature often contained insoluble parts which are probably caused by higher molar mass fractions or cross-linked nanoparticulate material, respectively. Thus, the molar masses derived from the chromatograms should be regarded as rather too low. As there was no significant difference between the results for different eluents, the data were determined from THF. A typical chromatogram comprising the elugrams for monomer, oligomer, and polymer is shown in Figure 3a. Both elugrams of the oligomer and the polymer display multiple well-resolved peaks which arise from monomer and shorter oligomers. With this knowledge, an internal calibration can be generated. This is especially intriguing because the sterically highly demanding adamantane groups might cause a strong deviation from the common standard polystyrene. For the elugram of the polymer a reasonable assignment of the peaks to the various oligomers can be made (see Figure 3b). The oligomer elugram shows some peaks and shoulders, which do not coincide with the corresponding signals of the polymer. We assume that they are caused by different end-groups which could have a significant effect on the elution volume for these rather short species.

In Figure 3b, a logarithmic dependence of the molecular weight on the elution time is seen in the calibration curves of the PS standard (blue solid line) and the internal calibration (red dashed line). The slightly smaller slope of the internal calibration compared to the polystyrene standards indicates a somewhat higher density for the adamantane comprising polymer. Assuming the linear dependence holds for higher masses, it is possible to determine the molecular weight averages for the corresponding polymers. Interestingly, the average degree of polymerization exceeds the values reported in the literature significantly although the synthesis and purification procedure was analogous.[10]

The formation of oligomers is also found in mass spectrometry. Classical methods for polymers with mild ionization methods like MALDI or ESI did not deliver signals that could be assigned to defined species from the polymer. Ionization by CI showed fragments up to pentamers besides unknown species (Figure S3).

The poly(1-vinyladamantane) synthesized in this work shows no melting transition, but in some samples, a weak glass transition T_g = 107 °C can be observed (see Figure S4). For the application as a template in nanodiamond synthesis, the decomposition temperature of the polymer is very important. Under a nitrogen atmosphere the decomposition process starts above 450 °C (see Figure S2). Slight losses up to

DOI: 10.1021/acsanm.8b01238
ACS Appl. Nano Mater. 2018, 1, 6073−6080

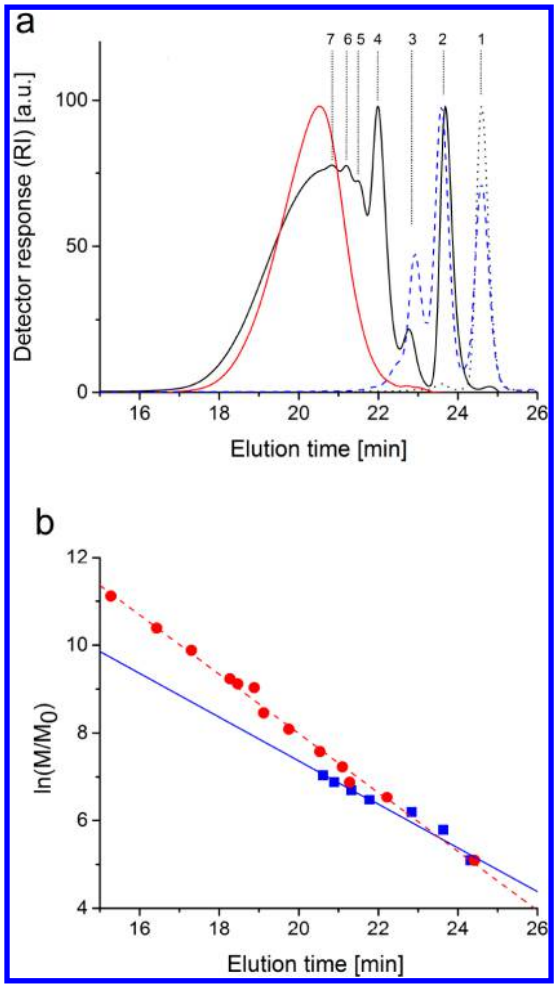

Figure 3. (a) Normalized GPC chromatograms of the monomer 1-vinyladamantane (black dots), an oligomer sample prepared with 10 mol % aluminum chloride at −78 °C (blue dashed), a polymer sample prepared with 10 mol % $AlBr_3$ at rt (black solid), and the polymer sample purified with further washing for nanodiamond seeding (red solid). The samples were injected as a 10 mg mL^{-1} solution in THF, and THF was used as eluent for the GPC measurement. The numbers indicate the degree of oligomerization. (b) Logarithmic display of the molecular weights of the standard calibration with polystyrene (red circles) and the internal calibration with poly(1-vinyladamantane) (blue squares) and their corresponding elution times. The molecular weights are divided by the standard molecular weight M_0 = 1 g mol^{-1}.

400 °C are assigned to water, traces of organic solvents, and small oligomers like dimers or trimers. Most likely the compounds evaporate, but no bonds are broken. Above 450 °C depolymerization is expected, but the adamantane units probably remain intact because they are thermally very stable[1] due to the tetrahedral linking of the carbon atoms. Explicit data on the thermal decomposition of adamantane in the gas phase cannot be found in the literature. The stability of the adamantane unit is supported by the mass spectra where no fragments of the tetrahedral cage can be found. The absence of melting transition in the DSC thermogram is indicative of an amorphous solid. A WAXS diffractogram (see Figure S5) indeed shows only broad signals supporting the presence of a disordered solid.

Nanodiamond Synthesis. One polymer sample with good yield and moderate molecular weight (M_n ca. 1500 g mol^{-1}, X_n ca. 9, yield 90%; see Table S1) was employed exemplarily as a template for nanodiamond growth following the literature.[21] As carbon source a mixture of (branched and unbranched) long alkanes was used. Tetramethylhydrazine was added to suppress the formation of graphite. The reaction was performed in a pressurized diamond anvil cell (DAC) at elevated temperatures. On the basis of the TGA results, we avoided in several experiments to exceed 275 °C to exclude thermal degradation of the polymer prior to diamond formation. The maximum temperature could be decreased to 200 °C, still leading to the formation of nanodiamonds (Figure 4c,d). After the nanodiamond (ND) growth is complete, the reaction solution was then transferred to a transmission electron microscope (TEM) grid. After thermal treatment up to 800 °C in the TEM microscope to remove residual organic material, many nanodiamonds were found. These NDs consist of two main fractions: one is very small, sub-10 nm, NDs, and the other is much larger, ca. 10−20 nm NDs. High-resolution TEM reveals that all the particles are crystalline (see Figure 4). The diffractogram of HRTEM images confirms that the crystalline products are mainly diamond plus a small amount of graphite or amorphorous carbon from the carbon film of the TEM grid. Without the polymer, much less diamond is generated (more than an order of magnitude less) which clearly demonstrates the template effect of the polymer. Interestingly, the larger objects were mostly polycrystalline (Figure 4b,c). This is to be compared to diamonds grown by the same procedure with nonpolymerized adamantane derivatives (Figure 4d) which produced mainly single crystals.[21] Hence, the characteristics of the polymer lead to polycrystalline structures of the nanodiamonds. This might be related to the number of adamantane moieties attached to each polymer chain and their different orientations.

Figure 5 displays a geometry-optimized structure of a decamer with two representations showing the different orientations of the adamantane groups and the bulkiness of the molecules. The latter will limit the flexibility of the chains, and the different orientations of the templating units therefore prevent single domain formation from one chain during the templated growth process. Dichloromethane (DCM) was added to the growth mix to dissolve the polymer in the low polar growth medium, where the concentration of DCM was chosen high enough to prevent visible precipitation of the polymer. We cannot exclude that besides nucleation of diamond nanoparticles by single chains, aggregates of multiple chains (see above) can act as nuclei, too. Shorter oligomers containing multiple adamantane species can also give a polycrystal diamond. Here we note that the diamond yield (fraction of template molecules that become diamond) is more than an order of magnitude higher with polymer templates than with nonpolymer adamantane derivatives.

■ CONCLUSION

During this work 1-vinyladamantane was successfully polymerized with different initiating systems. Adding to the already known polymerization with aluminum bromide, 1-vinyladamantane was polymerized with aluminum chloride and antimony[V] fluoride. Additionally, a convenient new initiator, $TiCl_2(OTf)_2$, for the cationic polymerization of sterically demanding vinylic monomers was found. Polymers with much higher molecular weights than those known in the literature were obtained. The molecular weight average reached up to 2400 g mol^{-1} (X_n = 15) as determined by GPC measurement in THF. The structure of the resulting polymeric material was

DOI: 10.1021/acsanm.8b01238
ACS Appl. Nano Mater. 2018, 1, 6073−6080

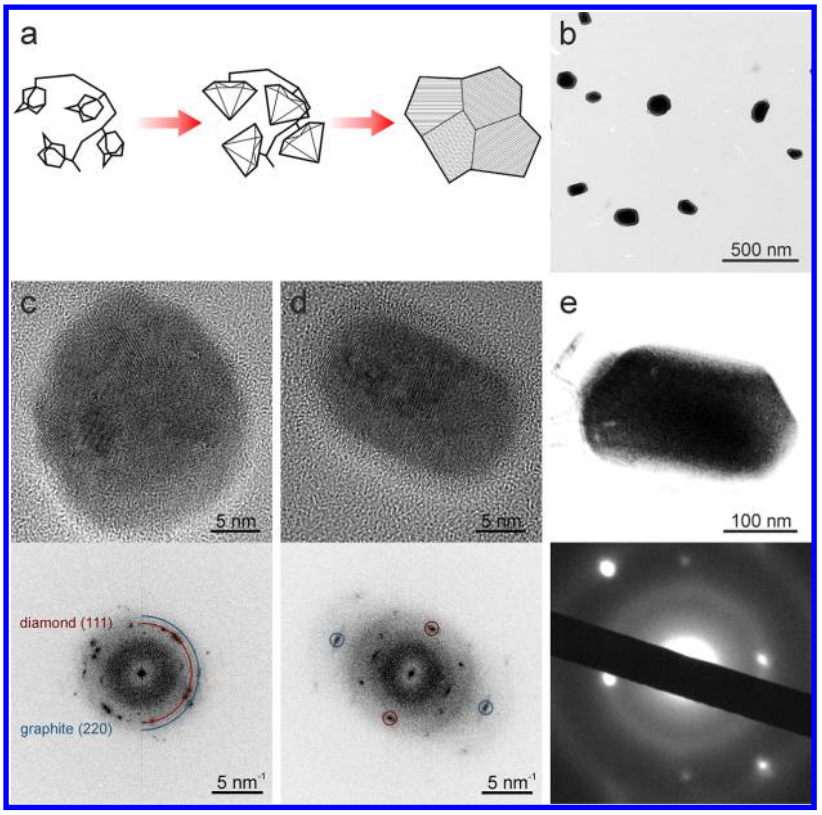

Figure 4. (a) Illustration of diamond growth from a polymer (here: tetramer) chain of linked adamantane molecules. Each molecule has a different orientation and produces diamonds of different orientation. Because the diamonds are so close together, they fuse into a single diamond but with regions having different lattice orientations. (b) Overview TEM image of nanodiamonds (T_{max} = 275 °C). (c) HRTEM image of a typical nanocrystal and its diffractogram showing the multiple orientation domains (T_{max} = 200 °C). The colored half-circles indicate the diamond 111 reflections at 4.9 nm^{-1} (red) and graphite 102 reflections at 5.6 nm^{-1} (blue). (d) HRTEM image showing a single-crystalline nanodiamond in [112] projection. The diamond 111 (4.9 nm^{-1}) and 220 (7.9 nm^{-1}) reflections are indicated by the red and blue circles, respectively (T_{max} = 200 °C). (e) Diamond grown from a single adamantane molecule in a different experiment. The diffraction pattern shows only one orientation.

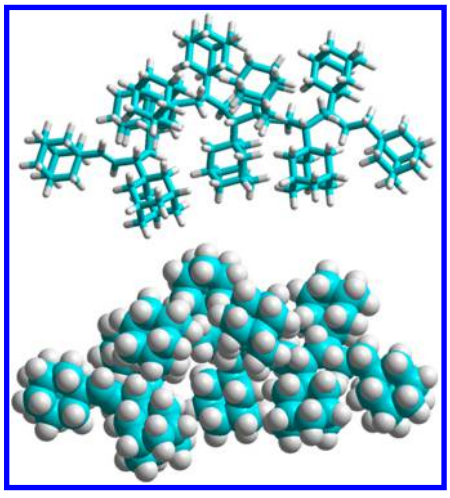

Figure 5. Decamer of poly(1-vinyladamantane) geometry optimized by semiempirical modeling (AM1) as rod and space-filling model.[29]

characterized by GPC, CI-MS, and NMR supporting the successful formation of the desired polymer structure with olefinic and potentially hydroxy end-groups present in some polymer chains. The thermal behavior was examined by DSC and TGA displaying a sufficiently high thermal stability for the production of nanodiamonds. The polymer was employed successfully as a template for nanodiamond growth. Interestingly, the 10−20 nm crystals that only appear when seeding with polymer were mostly multidomain structures. These are attributed to the different orientations of the single adamantane units and possibly the low flexibility of the polymer chains. The successful template effect for the nanodiamond synthesis is in accordance with the presence of the proposed polymer structure although traces of rearranged moieties or other side reactions cannot be fully excluded. It shall be mentioned that the synthesis could be performed at surprisingly low temperatures below 275 °C, which we attribute to the preorganization of the adamantane units in the polymer. Preliminary experiments have shown that the synthesis temperature could be decreased even further to 200 °C. Further work is dedicated to introduce defined numbers of heteroatoms, like nitrogen, silicon, or germanium, to finally produce closely spaced color centers like nitrogen, silicon, or germanium vacancies in diamond. These would enable more precise characterization of the crystals and are highly attractive for application as, for example, fluorescent sensors in biosystems. The rich chemistry of adamantane including the possibility to introduce heteroatoms makes this goal feasible. The high versatility of polymer chemistry allows for fine-tuning of the molecular structures. The template effect of these polymers for the synthesis of nanodiamonds is clearly superior to small molecule templates in terms of efficiency and synthesis conditions and shall open the field of tailored nanodiamond materials.

DOI: 10.1021/acsanm.8b01238
ACS Appl. Nano Mater. 2018, 1, 6073−6080

■ ASSOCIATED CONTENT

Supporting Information

The Supporting Information is available free of charge on the ACS Publications website at DOI: 10.1021/acsanm.8b01238.

Details of polymerization conditions (Tables S1 and S2); ^{1}H NMR spectra (Figure S1); IR spectrum (Figure S2); mass spectrum (Figure S3); kinetics; thermal analysis DSC (Figure S4), TGA (Figure S4); WAXS diffractogram (Figure S5) (PDF)

■ AUTHOR INFORMATION

Corresponding Author

*E-mail: ulrich.ziener@uni-ulm.de.

ORCID

Ulrich Ziener: 0000-0001-7582-1143

Present Address

M.H.A.A.: Center for Quantum Optics and Quantum Informatics, KACST, Riyadh 11442, Saudi Arabia.

Funding

R.L, H.Q., and U.K. thank the financial support by the DFG and the Ministry of Science, Research and the Arts (MWK) of Baden-Wuerttemberg in the framework of the "SALVE" (Sub-Angstrom Low-Voltage Electron Microscopy) project. P.H. acknowledges financial support from the Government of the Russian Federation (Mega-grant No. 14.W03.31.0028) and also by a grant from King Abdulaziz City for Science and Technology (KACST).

Notes

The authors declare no competing financial interest.

■ ACKNOWLEDGMENTS

The authors thank M. Zimmermann for technical support in the synthesis.

■ REFERENCES

(1) Dahl, J. E.; Liu, S. G.; Carlson, R. M. K. Isolation and Structure of Higher Diamondoids, Nanometer-Sized Diamond Molecules. *Science* **2003**, *299*, 96−99.

(2) Zhou, Y.; Brittain, A. D.; Kong, D.; Xiao, M.; Meng, Y.; Sun, L. Derivatization of Diamondoids for Functional Applications. *J. Mater. Chem. C* **2015**, *3*, 6947−6961.

(3) Wicora, M.; Brühne, K.; Fecht, H.-J. Synthesis of Nanodiamond. In *Carbon-Based Nanomaterials and Hybrids*; Fecht, H.-J., Brühne, K., Gluche, P., Eds.; Pan Stanford Publishing: Singapore, 2014; pp 5−48.

(4) Nakanishi, Y.; Omachi, H.; Fokina, N. A.; Schreiner, P. R.; Kitaura, R.; Dahl, J. E.; Carlson, R. M.; Shinohara, H. Template Synthesis of Linear-Chain Nanodiamonds inside Carbon Nanotubes from Bridgehead-Halogenated Diamantane Precursors. *Angew. Chem., Int. Ed.* **2015**, *54*, 10802−10806.

(5) Chen, Y.-C.; Chang, L. Chemical Vapor Deposition of Diamond on Silicon Substrates Coated with Adamantane in Glycol Chemical Solutions. *RSC Adv.* **2013**, *3*, 1514−1518.

(6) Chen, Y.-C.; Chang, L. Chemical Vapor Deposition of Diamond on an Adamantane-Coated Sapphire Substrate. *RSC Adv.* **2014**, *4*, 18945−18950.

(7) Tzeng, Y. K.; et al. Vertical-Substrate Mpcvd Epitaxial Nanodiamond Growth. *Nano Lett.* **2017**, *17*, 1489−1495.

(8) Terranova, M. L.; Rossi, M.; Tamburri, E. Nanocrystalline Sp 2 and Sp 3 Carbons: Cvd Synthesis and Applications. *Crystallogr. Rep.* **2016**, *61*, 897−906.

(9) Zuanic, M.; Majerski, Z.; Janović, Z. Poly(1-Vinyladamantane). *J. Polym. Sci., Polym. Lett. Ed.* **1981**, *19*, 387−389.

(10) Robello, D. R. Moderately High Refractive Index, Low Optical Dispersion Polymers with Pendant Diamondoids. *J. Appl. Polym. Sci.* **2013**, *127*, 96−103.

(11) Hasebe, T.; Kamigaito, M.; Sawamoto, M. Living Cationic Polymerization of Styrene with TiCl3(OiPr) as a Lewis Acid Activator. *Macromolecules* **1996**, *29*, 6100−6103.

(12) Riberio, M. R.; Portela, M. F.; Deffieux, A.; Cramail, H.; Rocha, M. F. Isospecific Homo- and Copolymerization of Styrene with Ethylene in the Presence of VCl3, AlCl3 as Catalyst. *Macromol. Rapid Commun.* **1996**, *17*, 461−469.

(13) Oh, J.-M.; Kang, S.-J.; Kwon, O.-S.; Choi, S.-K. Synthesis of ABA Triblock Copolymers of Styrene and p-Methylstyrene by Living Cationic Polymerization Using the Bifunctional Initiating System 1,4-Bis(1-Chloroethyl)Benzene/Snl4 in the Presence of 2,6-Di-tert-Butylpyridine. *Macromolecules* **1995**, *28*, 3015−3021.

(14) Satoh, K.; Nakashima, J.; Kamigaito, M.; Sawamoto, M. Novel BF3OEt2/R−OH Initiating System for Controlled Cationic Polymerization of Styrene in the Presence of Water. *Macromolecules* **2001**, *34*, 396−401.

(15) Vijayaraghavan, R.; MacFarlane, D. R. Organoborate Acids as Initiators for Cationic Polymerization of Styrene in an Ionic Liquid Medium. *Macromolecules* **2007**, *40*, 6515−6520.

(16) Mitu, S.; Baird, M. C. Isobutene Polymerization Induced by Adducts of B(C(6)F(5))(3) with Carboxylic Acids CH(3)(CH(2))-(N)CO(2)H (n = 2,4,6,8,10,12,14,16,18,20); Chain Length Effects on This Strong Acid, Carbocationic Polymerization Initiating System. *Eur. Polym. J.* **2006**, *42*, 2039−2044.

(17) Lechner, M. D.; Gehrke, K.; Nordmeier, E. H. *Makromolekulare Chemie*; Birkhäuser: Basel, 2010.

(18) Perrin, D. D.; Armarego, W. L. F. *Purification of Laboratory Chemicals*; Pergamon: Oxford, 1988.

(19) Fokin, A. A.; Butova, E. D.; Barabash, A. V.; Huu, N. N.; Tkachenko, B. A.; Fokina, N. A.; Schreiner, P. R. Preparative Synthesis of Vinyl Diamondoids. *Synth. Commun.* **2013**, *43*, 1772−1777.

(20) Schmeißer, M.; Sartori, P.; Lippsmeier, B. Zur Chemie Der Perfluoralkansulfonsäuren. *Chem. Ber.* **1970**, *103*, 868−879.

(21) Zapata, T.; et al. Organic Nanodiamonds. arXiv:1702.06854 [physics.chem-ph].

(22) Böhrer, H.; Trapp, N.; Himmel, D.; Schleep, M.; Krossing, I. From Unsuccessful H2-Activation with Flps Containing B(Ohfip)3 to a Systematic Evaluation of the Lewis Acidity of 33 Lewis Acids Based on Fluoride, Chloride, Hydride and Methyl Ion Affinities. *Dalton Trans.* **2015**, *44*, 7489−99.

(23) Pepper, D. C.; Reilly, P. J. Chain Propagation Constants in the Cationic Polymerization of Styrene. *J. Polym. Sci.* **1962**, *58*, 639−647.

(24) Okamura, S.; Kanoh, N.; Higashimura, T. Rate Constant of Propagation Reaction in Stationary State of Cationic Polymerization. *Makromol. Chem.* **1961**, *47*, 19−34.

(25) Fort, R. C.; Schleyer, P. v. R. Adamantane: Consequences of the Diamondoid Structure. *Chem. Rev.* **1964**, *64*, 277−300.

(26) Anderson, J. E.; de Meijere, A.; Kozhushkov, S. I.; Lunazzi, L.; Mazzanti, A. Conformational Studies by Dynamic NMR. 95. Rotation around the Adamantyl-Alkyl Bond. Remote Substituent Effect on Conformational Equilibrium. *J. Org. Chem.* **2003**, *68*, 8494−8499.

(27) Kostjuk, S. V.; Yeong, H. Y.; Voit, B. Cationic Polymerization of Isobutylene at Room Temperature. *J. Polym. Sci., Part A: Polym. Chem.* **2013**, *51*, 471−486.

(28) Jaacks, V.; Frank, H.; Grünberger, E.; Kern, W. The Mechanism of Hydride Transfer in Cationic Polymerization of Trioxane. *Makromol. Chem.* **1968**, *115*, 290−295.

(29) Hyperchem 8.0; Hypercube Inc., 2007.

DOI: 10.1021/acsanm.8b01238
ACS Appl. Nano Mater. 2018, 1, 6073−6080